IEEE Access
Multidisciplinary ⋮ Rapid Review ⋮ Open Access Journal

Received December 21, 2020, accepted January 10, 2021, date of publication January 14, 2021,
date of current version January 22, 2021.

Digital Object Identifier 10.1109/ACCESS.2021.3051646

Blind System Identification in Noise Using a Dynamic-Based Estimator

SUMONA MUKHOPADHYAY[1], BOYUAN LI[2], AND HENRY LEUNG[2], (Fellow, IEEE)
[1]Department of Electrical Engineering and Computer Science, York University, Toronto, ON M3J 1P3, Canada
[2]Department of Electrical and Computer Engineering, University of Calgary, Calgary, AB T2N 1N4, Canada

Corresponding author: Sumona Mukhopadhyay (mukhopas@yorku.ca)

ABSTRACT In this work we consider the problem of blind system identification in noise driven by an independent and identically distributed (i.i.d) non-Gaussian signal generated from a deterministic nonlinear chaotic system. A new estimator for the phase space volume (PSV) which is a dynamic-based property of chaos is derived using the maximum likelihood formulation. This novel estimator of PSV is denoted as the maximum likelihood phase space volume (ML-PSV). The Cramér Rao Lower Bound (CRLB) of the ML-PSV estimator has also been derived. We have shown that the mean square error of the ML-PSV estimate gradually approaches its CRLB asymptotically. An algorithm is formulated that applies the ML-PSV estimator as an objective function in the task of blind system identification of autoregressive (AR) and moving average (MA) models. The proposed technique is shown to improve blind identification performance at low signal-to-noise ratio (SNR) when the system is driven by both chaotic numeric and symbolic signals. The efficiency of our proposed method is compared with conventional blind identification methods through simulations. Our technique is further validated through experimental evaluation based on a software defined radio (SDR). Results show that the ML-PSV method outperforms the existing blind identification methods producing estimates at a low SNR of $\leq$ 20 dB.

INDEX TERMS Chaos, nonlinear dynamics, maximum likelihood, Cramér Rao lower bound (CRLB), blind system identification, symbolic dynamics, software defined radio.

I. INTRODUCTION

The task of system identification involves the design of the input probing signal or driving signal [1], [2]. One of the application areas of system identification is in channel equalization where it is desired to identify the channel without any access to the input signal [3]–[7]. This technique of identifying the channel without the availability of the input information is a blind system identification problem [8]. In blind identification, the input signal as well as the propagation channel parameters are unknown at the receiver.

There has been a growing interest in the use of chaotic signals in many applications such as chaos-based equalization [9]–[13], communications [14]–[19], and control [20]–[23]. A chaotic signal is characterised by a nonlinear map with sensitivity to initial conditions. Chaotic signals have a broad-band spectrum similar to white noise that can be used to excite a system for identification purpose. It is easier to generate chaotic signals with the advancements in analog circuits. Also, chaotic signals are deterministic, which suggests that they can be controlled by synchronization [24]. The deterministic characteristic of chaotic signals is an added advantage over white Gaussian noise (WGN) signals due to which the entire signal can be generated from only its initial condition. As such, chaotic signals are relatively easy to implement and analyze unlike WGN signals. Furthermore, past researchers have shown that when chaos is used as the driving signal, blind system identification performance of the chaotic method is similar to the nonblind least squares (LS) method [25]. Based on these merits chaotic signals can be an ideal choice for the design of the driving signal in system identification and finds its application in blind channel equalization.

There are various approaches to blind identification using chaos. The traditional approach was the maximum likelihood (ML) approach [26] which gave suboptimal performance at a certain range of SNR and suffered from threshold effect achieving the CRLB at a high SNR >= 20 dB [27].

The associate editor coordinating the review of this manuscript and approving it for publication was Easter Selvan Suviseshamuthu.

Another technique for chaos-based system identification is the inverse filtering approach. This technique involves estimation of the system coefficients by minimizing an objective function of the output of an inverse system. The minimum phase space volume (MPSV) technique for blind system identification using chaos is an estimation method that applies the inverse filtering approach [9], [28]. The basic idea of MPSV procedure is that a chaotic signal has a finite volume in phase space (PSV) which is a characteristic unique to chaotic signals. The MPSV method works by minimizing the phase space volume (PSV) property of the output of an inverse filter, which causes the parameters of the inverse filter to converge to the correct values of the signal. The MPSV estimation technique can be applied to random signals such as WGN [29]. The authors have used the concept called abstract dynamical system to model any process. It is a generalization of the chaos approach where PSV can be defined for random process. However, for a case such as additive White Gaussian noise (AWGN), it becomes a very high dimensional dynamical system and computing PSV becomes time consuming. Therefore, PSV is more suitable for low dimensional system like chaos but it works in principle for AWGN. The MPSV estimator requires a short data in comparison to least squares (LS). However, its computational load is very heavy and gives poor identification results at low SNR. Another method for chaos-based blind system identification using the inverse filtering approach is the minimum nonlinear prediction error method (MNPE) [30]. The MNPE is a nonlinear predictor that applies the short-term predictability property unique to chaos. Based on the short-term predictability of chaos, the received signal is passed through an inverse filter and the system parameters are estimated by minimizing the nonlinear prediction error (NPE) of the inverse filter output. The MNPE estimation method is shown to achieve superior identification performance at high SNR. However a major drawback of the MNPE estimator is its poor performance at low SNR. However, based on the inverse filtering approach, it was shown that when chaos is used as the driving signal, blind identification can be accurate when compared to the optimal nonblind approach based on WGN input signal used with the LS estimator [25], [31].

Another approach for chaos-based blind system identification is the state-space representation by applying the Expectation Maximization and Unscented Kalman filtering (EM-UKF) technique [32]. Using this approach it was proved that the CRLB of blind identification with chaos is the same as that of the CRLB of nonblind identification using WGN. Although, the state space format is convenient for estimation, the estimates are not as accurate as the optimal nonblind LS at low SNR. Recently, a chaos-based blind identification method applying the state-space with EM-UKS estimator was proposed for general signals, and the CRLB was derived for the chaos representation [12]. This technique employs the entropy and deterministic properties of chaos to achieve blind identification performance close to nonblind LS estimator. A primary challenge encountered in blind system identification using chaos is that existing methods perform poorly at low SNR [33], [34]. Nevertheless, the above mentioned approaches for chaos-based blind system identification suggest that by exploiting certain unique characteristics of chaos such as the PSV, short-term predictability, entropy and determinism, blind identification performance using chaos achieves performance comparable to the statistically optimal nonblind LS using WGN. Thus, chaotic signals could be an ideal candidate for blind identification.

Our proposed method tries to address the issue of blind identification performance of the MPSV method at low SNR. In this work, we propose a new formulation of the PSV by directly incorporating the WGN in the formulation and use ML formulation of PSV to maximize the performance of the PSV estimator in a noisy environment. Our proposed technique for improving the MPSV method is called as the ML-PSV method. An algorithm is designed to apply the ML-PSV estimate for blind system identification using chaotic signals. We further improve the performance of the ML-PSV approach using symbolic dynamics. Chaotic signals can either be used as chaotic numerical (CN) signal (which is a real valued time series signal generated from the output of a chaotic dynamical system) or as chaotic symbolic (CS) signal [35]. A symbolic time series signal can be obtained by discretizing or partitioning the CN time series using the method of symbolic dynamics [36]. By the method of symbolic dynamics a chaotic time series can be partitioned into a finite set of disjoint regions and assigned a unique symbol to each region. Instead of representing a signal by its numeric values of its signal points, one watches the progression of symbols corresponding to the alternation of the numbers as the system evolves with time. For example, in the case of 1D chaotic Tent map whose time series lies in the interval [0,1], its CN signal is partitioned into 2 segments: [0, 0.5) which is assigned a symbol of -1 and the region [0.5, 1) is assigned a symbol of $+1$. This technique can extract hidden features like the occurrence of frequent recurrent patterns [37], [38]. Even though some details of the dynamics may be lost due to the symbolization, most of the temporal correlations remain embedded in the structure of the symbol sequence and most importantly, the advantages of symbolization are ease of computation and robustness against noise [39]. In this work, two partitions are applied to create a binary valued chaotic symbolic (CS) time series. We further extend the ML-PSV method to blind system identification using CS input signals to improve the blind identification performance at low SNR.

The physical problem that we are trying to address is equalization for wireless communication which is required in order to mitigate the effect of intersymbol interference (ISI) [40]–[43]. Traditionally, blind equalization is achieved by using higher order statistics (HOS) [44]. These HOS based methods perform well in suppressing Gaussian noise but are sensitive to parameter settings, having slow convergence, and requiring large amounts of data. Meanwhile, methods based on subspace [3], [45] obtain more accurate estimation results at high SNRs but perform poorly at low SNRs.

Furthermore, subspace-based methods [46] are sensitive to parameter estimation errors. For example, the performance of these methods relies on the accurate estimation of the channel order. A small error in the channel order estimation may cause the estimation performance to produce large errors. In this work, the choice of the models are Autoregressive (AR) and Moving Average (MA) models. An MA model is usually considered for channel equalization and is also used as an approximation to reduce the order. We have validated our proposed approach through experimental evaluation for blind channel equalization where the MA components represent a finite impulse response (FIR) system. Our novel research contributions are highlighted below:

- We have derived a new technique called as the ML-PSV using maximum likelihood formulation for estimating the phase space volume (PSV) of a dynamical system.
- The CRLB of the ML-PSV estimator is derived. It is shown that the mean square error (MSE) of the ML estimate of PSV gradually approaches its CRLB.
- The derived ML-PSV estimator is applied in an algorithm as an objective function for improving blind system identification performance using chaos. Results prove that the ML-PSV estimator suppresses the impact of measurement noise so that the ML-PSV estimate converges to yield the true coefficients of the system.
- We evaluate the efficiency of ML-PSV in blind system identification task using CN and CS signals. Overall, the performance of our method using CS signal in blind system identification is better than CN signal.
- The ML-PSV estimator for blind identification achieves performance comparable to nonblind LS at a low SNR of $\leq$ 20 dB and is also computationally inexpensive in comparison to the MPSV technique.
- Our approach is validated through experimental evaluation which are the first experimental results demonstrating the practicality of chaos-based channel equalization to the best of our knowledge.

The rest of the paper is organized as follows. Section II describes the background and motivation for our methodology. In Section III the ML formulation of PSV and its CRLB are derived. In Section IV an algorithm for blind system identification is presented where the ML-PSV estimator is applied forblind identification of AR and MA models. Simulation results are also presented to evaluate the performance of the proposed ML-PSV method. In Section V the SDR experiments are used to illustrate the effectiveness of the ML-PSV method in equalizing a real wireless communication channel. Conclusion is given in Section VI.

II. RESEARCH BACKGROUND AND MOTIVATION

This section describes the background that is required for developing the proposed new formulation for phase space volume and its application to blind identification. The background areas are the phase space reconstruction and the existing MPSV technique. We then present the motivation for improving MPSV technique.

A. EMBEDDING THEORY FOR PHASE-SPACE RECONSTRUCTION

Consider a discrete dynamical system in the form of:

$$x_{n+1} = f(x_n), \tag{1}$$

where $\mathbf{x} = [x_1, x_2, \ldots, x_n]^{\mathsf{T}}$ is the system's state vector, $f(\cdot)$ is a nonlinear map, and $\mathbf{x}_n$, $n = 0, 1, 2, \ldots$ is the trajectory of the system. At any given time a dynamical system has a state given by a set of real numbers (a vector) which can be represented by a point in the state space or phase space. The phase space is the space of all possible states of the system i.e, the phase space is the number of dynamical variables of the system. The state space reconstruction method aims to reconstruct the state vectors from the time series, so that the time evolution of these vectors replicates a dynamics equivalent to that of the original system. Starting from the initial value x_0, the trajectory $\mathbf{x}_n$ describes the evolution of the system along time. After transient dynamics, the system's bounded trajectory will converge to an attractor, i.e., a bounded invariant set $\mathcal{A}$. The dynamics is constrained in a compact manifold $\mathcal{M}$ containing the attractor $\mathcal{A}$. The time evolution corresponding with an initial value $x_0 \in \mathcal{M}$ is denoted by $\mathbf{x}_n = f^n(x_0)$. Intuitively, to study the property of the attractor in the state space, the values of all the system's state components should be known. However, Takens' embedding theory [47] implies that from a few or even one single time series observed from the system, it is possible to study the dynamical property of the whole system, i.e., the system can be reconstructed by observations. By sampling the time series of only single coordinate x_n, a variety of independent coordinate sets can be obtained such as $[x_n, x_{n-\tau}, x_{n-(D_E-1)\tau}]$ is a phase space reconstruction of the original system. Thus a multidimensional phase space can be reconstructed and such a reconstruction implies that the one dimensional observed time series can contain all the information of the dynamics of the whole original system. Here τ is the sampling interval alternately known as the delay and D_E is the embedding dimension.

The geometry of the attractor will be quite similar to that of the original system for a proper choice of the parameters for embedding such as the delay and the embedding dimension. In essence an embedding means a a similarity transformation of the coordinates having a one-to-one property between the original system and the reconstructed system [48]. This is an essential property because the state of a deterministic dynamical system, as well as its future evolution, are completely specified by a point in the state space. Therefore, the delay coordinate map actually sets up a bridge between the dynamics of the original system and the dynamics in the reconstructed space [49]. Theoretically, an embedding of the original time series can be obtained for $D_E \geq 2m + 1$ where m is the intrinsic or the actual dimension of the system. Moreover, the embedding theory implies that the dynamics in the reconstructed space is topologically conjugated with the dynamics in the original state space. Thus, the nonlinear dynamic properties such as Lyapunov exponent (LE), entropy, PSV are preserved from the original system to the

reconstructed system, which forms the cornerstone of the state space reconstruction technique. The strong Whitney's embedding theorem provides the choice for the embedding dimension D_E and proved that the embedding dimension $D_E = 2m$. Such a choice yields a one-to-one correspondence between the reconstructed phase space and the real system. The advantage of phase space reconstruction is that by using limited data, one can reconstruct the phase space such that the properties of the original system are preserved. From a sequence of scalar measurements, we can reconstruct every state vector, in a D_E-dimensional phase space, following the delay method.

B. THE MINIMUM PHASE SPACE VOLUME APPROACH FOR PARAMETER ESTIMATION

According to Takens' embedding theorem time delay reconstruction can be used to reconstruct the dynamics of a chaotic attractor. We can work in the reconstructed time delay space and learn essentially as much as we could from the true state space provided that the embedding dimension is sufficient to unfold the attractor. The parameters of a system that is driven by a chaotic signal can be obtained by minimizing the dynamic property of chaos known as the Phase Space Volume (PSV). To do so, the received signal is first passed through an inverse filter, and the parameters are estimated by minimizing the ''volume'' of the output signal of the inverse filter in an embedded phase space. The basic idea is that the signal is attracted to stay in finite dimensional attractor manifold and, hence, has a finite ''volume'' in an embedded phase space. On the other hand, a random signal does not have any regular behavior in any finite dimensional phase space and hence, its ''volume'' is expected to be relatively large.

The problem of blind identification analyzed in this paper is formulated as:

$$y_n = z_n(h) + x_n + v_n \tag{2}$$

where z_n is the signal of interest, x_n is a chaotic signal and v_n is additive noise, $n = 1, \ldots, N$. The problem is to identify the parameter h by analyzing the measures signal y_n. This can be done by applying the PSV as an optimization function expressed in terms of the measured signal y_n. It was shown in [9] that the correct value of parameter h could be estimated by PSV minimization of the inversely filtered signal:

$$u_n = y_n - z_n(\hat{h}) = z_n(h) - z_n(\hat{h}) + x_n + v_n. \tag{3}$$

We summarize the MPSV method for parameter estimation in Algorithm 1:

C. MOTIVATION

The MPSV approach described above suffers from two issues: (a) poor noise performance and (b) high computational complexity of N^2 multiplications to calculate each volume as per (4). This prohibits the real-time application of PSV approach. For example in channel equalization, a fast estimation of channel coefficients is necessary. Otherwise, during the calculating process, the channel coefficients may have changed already. Then the estimation result is not correct in that way. We focus on developing a new formulation for (4) in an attempt to improve the blind identification performance of the PSV approach at low SNR and to reduce the complexity for a single volume calculation.

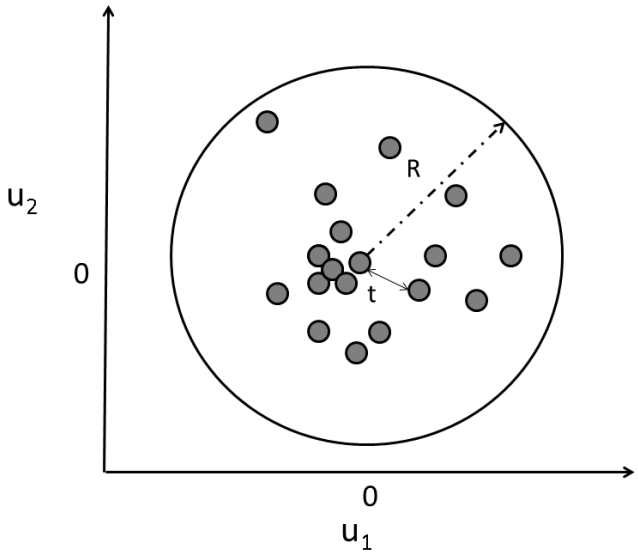

FIGURE 1. Volume of the sphere with radius R, distance between points t and embedding dimension $D_E = 2$.

III. PROPOSED METHODOLOGY: MAXIMUM LIKELIHOOD ESTIMATION OF PHASE SPACE VOLUME

In this section the ML estimate of the PSV is derived along with its CRLB. The starting point of our method is the state-space or phase space reconstruction for which the embedding theory is applied.

A. DERIVATION OF ML-PSV ESTIMATOR

The starting point in the derivation of the PSV estimate using maximum likelihood (ML) approach is to delay embed an observed univariate time series given by $u_1, u_2, \ldots, u_n, \ldots, u_N$, by using Takens' time delay embedding technique. This method obtains vectors of the form $\mathbf{u}_n$ by stacking D_E previous entries of the time series u_n samples uniformly in time with sampling time τ (known as delay) up into a vector:

$$\mathbf{u}_n = [u_n, u_{(n-\tau)}, \ldots, u_{(n-(D_E-1)\tau)}]^{\mathsf{T}}. \tag{5}$$

The ML approach to estimate the PSV is inspired by estimation technique of the intrinsic dimension m [50] by the principle of ML to the distances between close neighbors, and derived the estimator m by a Poisson process approximation. Figure 1 shows a pictorial representation of the volume of sphere centered around a data point $\mathbf{u}_n$ in the embedded phase space D_E. State space reconstruction is a fundamental step before the analysis of a time series in terms of dynamical systems theory. The process which counts the number of points falling into a higher dimensional sphere is

Algorithm 1 Algorithm for Blind System Identification Using MPSV

1: Given the received signal $y_n, n = 1, 2, \ldots, N$, construct an inverse system u_n where the parameter vector $\hat{\mathbf{h}}$ is the estimate of the true parameters $\mathbf{h}$.
2: Embed u_n into a D_E dimensional phase space using the delay coordinate, i.e., $\mathbf{u}_n = (u_n, u_{n+\tau}, \ldots, u_{n+(D_E-1)\tau})$ is an embedding dimension of the chaotic map $f(\cdot)$. (In this work, $\tau = 1$).
3: Minimize the PSV of the inverse filter output vector $\mathbf{u}_n$ i.e.,

$$\begin{aligned}\hat{h} &= \min V(\mathbf{u}_n), \\ &= \min_{\hat{h}} \sum_{i=1}^{N-D_E+1} \min_{j\neq i} |u_i - u_j| \times \ldots \times |u_{i+D_E-1} - u_{j+D_E-1}| \end{aligned} \tag{4}$$

a binomial process. λ is the average count of points falling inside the small sphere. Since the sphere radius R is small, the probability of a point falling into the sphere is small. When the sample number N is large, the binomial process can be approximated by a Poisson process. This is the rationale for modelling the process with the Poisson distribution. The approach of estimating the intrinsic dimension is based on estimating the local dimension of a point cloud data which is the representation of data points in phase space. A similar approach is used here to estimate the volume of data in phase space.

Data in high dimension, D_E are denoted by *i.i.d* samples, $\mathbf{U} = \{\mathbf{u}_1, \ldots, \mathbf{u}_n, \ldots, \mathbf{u}_N \in \mathbb{R}^{D_E}\}$ obtained from the Takens' delay embedding in (5) where a data point is represented by $\mathbf{u}_n \in \mathbb{R}^{D_E}$. In Figure 1 a small sphere of radius R is considered and $\mathbf{u} \in \mathbb{R}^{D_E}$ denotes a point inside the sphere with t as the nearest neighbor Euclidean distance from $\mathbf{u}$ to its k^{th} nearest neighbor. The derivation is based on the assumption that close neighbors in $\mathbb{R}^m$ are mapped to close neighbors in the D_E-dimensional space.

The proposed approach for estimating the ML estimate of the PSV is based on the idea that if we sample $\mathbf{u}_1, \mathbf{u}_2, \ldots, \mathbf{u}_n, \ldots, \mathbf{u}_N$ (N is fixed) from a D_E- higher-dimensional space which are *i.i.d* from a density $p(\mathbf{u})$, the proportion of points that fall into a ball around a point is $\frac{k}{N} \approx p(\mathbf{u})V(m)t(\mathbf{u})^m$, where V is the volume of a sphere with radius R. The volume V of an m dimensional object embedded in D_E dimension scales with its intrinsic dimension m is described as:

$$V = V(m)t^m \tag{6}$$

where $V(m)$ is the volume of the sphere in $\mathbb{R}^m$ and where t represents the Euclidean distance between points. Considering $\aleph(\cdot)$ as the process which counts the number of points falling into a small D_E higher dimensional sphere $B(R, \mathbf{u})$ of radius R centered around a point. Assume that, $N \to \infty$, $k \to \infty$ and $\frac{k}{N} \to 0$, $p(\mathbf{u})$ is constant inside the sphere for a small R where R lies between the range r_1 and r_2, the rate λ of the counting process $\aleph(\cdot)$ can be written as:

$$\lambda = p(\mathbf{u})V(m)mt^{m-1} \tag{7}$$

The log-likelihood of the process $\aleph(t)$ which counts observations within distance t from a point is then given by:

$$\begin{aligned}\ell(V) &= p(\aleph(t)|V), \\ &= \int_{r_1}^{r_2} \ln\lambda d\aleph(t) - \int_{r_1}^{r_2} \lambda dt \end{aligned} \tag{8}$$

where $r_1 < r_2$ denote the lower and upper limits for the radius. We have,

$$\begin{aligned}&\ell(V) \\ &= \int_{r_1}^{r_2} \ln(p(\mathbf{u})V(m)mt^{m-1}) d\aleph(t) \\ &\quad - \int_{r_1}^{r_2} (p(\mathbf{u})V(m)mt^{m-1})dt, \end{aligned} \tag{9}$$

$$\begin{aligned}&= \int_{r_1}^{r_2} \ln(\exp(\theta)\frac{V}{t^m}mt^{m-1}) d\aleph(t) \\ &\quad - \int_{r_1}^{r_2} (\exp(\theta)\frac{V}{t^m}mt^{m-1})dt, \end{aligned} \tag{10}$$

$$= \int_{r_1}^{r_2} \ln(\exp(\theta)Vmt^{-1}) d\aleph(t) - \exp(\theta)Vm\int_{r_1}^{r_2} \frac{t^{m-1}}{t^m} dt, \tag{11}$$

$$= \int_{r_1}^{r_2} (\theta + \ln V - \ln t + \ln m) d\aleph(t) - \exp(\theta)mV\int_{r_1}^{r_2} \frac{1}{t} d(t), \tag{12}$$

In practice,

$$\begin{aligned}&= (\theta + \ln V - \ln t + \ln m)[\aleph(r_2) - \aleph(r_1)] \\ &\quad - \exp(\theta)mV[\ln r_2 - \ln r_1]. \end{aligned} \tag{13}$$

$$\begin{aligned}&= (\theta + \ln V - \ln t + \ln m)[\aleph(r_2) - \aleph(r_1)] \\ &\quad - \exp(\theta)mV[\ln(r_2/r_1)]. \end{aligned} \tag{14}$$

where let $\ln T = \ln(r_2/r_1)$ which in practice denotes the logarithm of the Euclidean distance matrix, $p(\mathbf{u}) = \exp(\theta)$, $\ln p(\mathbf{u}) = \theta$[1] The ML estimator for PSV is given by:

$$\hat{V_{ML}} = \arg\max \ell(V) \tag{15}$$

[1]We have used $p(\mathbf{u}) = \exp(\theta)$ in order to simplify $\ln(p(\mathbf{u}))$ to θ and get rid of θ when computing the derivative of the likelihood function. Thus, we have $\ln(\exp(\theta)) = \theta$ and $\theta' = 0$ since θ is a constant.

Differentiating the log likelihood with respect to V and equating to zero:

$$\frac{\partial \ell(V)}{\partial V} = 0, \tag{16}$$

$$\frac{\aleph(r_2) - \aleph(r_1)}{V} - m\exp(\theta)[\ln T] = 0 \tag{17}$$

$$\hat{V} = \frac{\aleph(r_2) - \aleph(r_1)}{m\exp(\theta)[\ln T]} \tag{18}$$

which is the ML estimator of the PSV based on the distances to all the neighbors of a single point and $\aleph(r_1)$ and $\aleph(r_2)$ denotes the count of the number of points. The values of r_1 and r_2 have been determined by experiments and explained subsequently. To combine the results obtained in the neighborhood of all N data points to give a single inference of PSV, we can average $\hat{V}(\mathbf{u})$. Thus, the ML estimator for PSV can be expressed by,

$$\hat{V}_{ML} = \frac{\sum_{n=1}^{N} \hat{V}(\mathbf{u}_n)}{N}. \tag{19}$$

B. REDUCTION IN COMPLEXITY

The time complexity of our proposed ML-PSV is significantly reduced due to the ML formulation for calculating the PSV instead of the formulation in (4). The calculation of ML on the inverse filter output of length N has a complexity of $O(N)$ along with a sorting algorithm to find the minimum ML-PSV which has a complexity of $O(N \log N)$. So the total complexity for calculating a single volume using the new formulation of PSV in (19) is $O(N + N \log N)$.

C. DERIVATION OF CRAMÉR RAO LOWER BOUND AND ITS PROPERTIES

The efficiency of $\hat{V}_{ML}$ can be assessed by the CRLB which is the inverse of the Fisher information (FI) $J(V)$ expressed as:

$$var(\hat{V}_{ML} - V) \geq [J(V)]^{-1} \tag{20}$$

where

$$[J(V)] = -E\left[\frac{\partial^2 \ell(V)}{\partial V^2}\right] \tag{21}$$

CRLB serves as the lower bound for the estimation performance of any unbiased estimator. Let, $D = \aleph(r_2) - \aleph(r_1)$. Computing the second order derivatives from (19):

$$\frac{\partial^2 \ell(V)}{\partial V^2} = \frac{-D}{V^2} \tag{22}$$

$$\begin{aligned}[J(V)] &= \frac{-E\Big[-D\Big]}{V^2} \\ &= E[D]\frac{1}{V^2} \\ &= \frac{\lambda}{V^2}\end{aligned} \tag{23}$$

where V is deterministic. The variance of the estimator error is given by,

$$\begin{aligned}var(\hat{V}_{ML}) &= E\left[\frac{1}{N}\sum_{n=1}^{N}\hat{V}(\mathbf{u}_n) - E[\hat{V}_{ML}]\right]^2 \\ &= \frac{1}{N^2}\sum_{n=1}^{N} E\left[\hat{V}(\mathbf{u}_n) - V\right]^2\end{aligned} \tag{24}$$

and assuming that the estimator is unbiased. Since, $var(\hat{V}_{ML}) \geq \frac{1}{J(V)}$, we can conclude that the estimator is *efficient* and the efficiency of the estimator is,

$$var(\hat{V}_{ML}) \geq \frac{V^2}{\lambda} \tag{25}$$

IV. APPLICATION OF ML-PSV TO BLIND SYSTEM IDENTIFICATION

It has been proven in [9] that as the PSV occupied by the output signal goes to the minimum, the parameters of the inverse filter approach the correct parameters of the signal to be estimated. Purely random signals however do not have any regular behavior in finite low dimensional phase space and hence its volume is expected to be relatively large. It is to be noted that when x_n is used to drive a system, the system output y_n has been shown to have an embedding dimension of $D_E = L + m$ where m is the intrinsic dimension of the chaotic system [51].

The following theorem supports our claim of applying the ML-PSV as an objective function, minimizing it with respect to the inverse filter coefficients $\hat{h}$ is expected to set the parameter vector $\hat{h}$ of the inverse filter to converge to the true value h. This is feasible when the proposed blind identification procedure using ML-PSV works in noise to suppress the impact of v_n on u_n so that the ML-PSV estimate converges to the true value as $N \to \infty$.

Theorem: Given the inverse filter output u_n the ML-PSV estimate yields the true parameters corresponding to the minimal ML-PSV estimate value of the inverse filter output in presence of noise i.e., $\mathbf{h} = \hat{\mathbf{h}}$ if and only if $V_{ML}(u_n)$ is minimum.

Proof: ML-PSV estimate is calculated from the output of the inverse filter which is a time series,

$$u_n = \{u_1, u_2, \ldots, u_n, \ldots\}. \tag{26}$$

The output of the above inverse filter is delay embedded using Takens' delay embedding that can construct a vector $\mathbf{u}_n$ containing as entries time delayed expressions of u_n expressed in the form:

$$\mathbf{u}_n = [u_n, u_{(n-\tau)}, \ldots, u_{(n-(D_E-1)\tau)}]^{\mathsf{T}}. \tag{27}$$

where τ is the delay time and D_E is the embedding dimension of the data where $D_E \geq 2m + 1$. This enables one to work in the reconstructed time delay space and learn essentially as much as we can from the true state space provided that the embedding dimension is sufficient enough to capture the dynamics of the system. ML-PSV quantifies the amount of

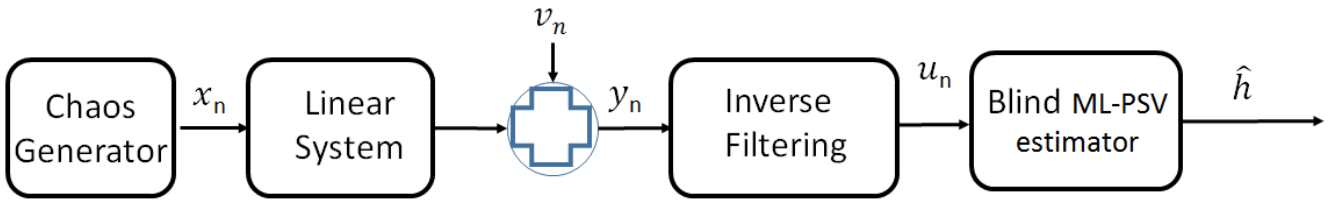

FIGURE 2. Schematic diagram of the proposed blind system identification approach.

data points occupied in a fixed region in this reconstructed phase space. It counts the number of data points falling within r_1 and r_2. The distance between two reconstructed vectors in a D_E-dimensional phase space can be calculated using the Euclidean norm as $T = ||\mathbf{u}_p - \mathbf{u}_q||$ in phase space for $p \neq q$.

When a system is corrupted with white noise, it fills densely the phase space so the divergence between close initially points becomes infinite or large. Under ideal conditions and perfect estimation, the output of the inverse filter $u_n = x_n$. Let us consider a dynamic system $f(\cdot)$ and v_n is a measurement noise of zero mean and unity variance. Thus we have,

$$u_n^v = f(u_{n-1}) + v_n, \tag{28}$$

Now,

$$||u^v - f(u)|| \geq ||u - f(u)||, \tag{29}$$

where u is the noiseless system when $v = 0$. Then we have,

$$T \leq T^v. \tag{30}$$

This means that the separation between two nearby points is more in the presence of noise as the data points are dispersed in phase space and hence the distance for the noiseless systems T is lesser than that of its noisy counterpart T^v. So, if noise is reduced then it would imply that nearby points come closer resulting in the compactness of the phase space and hence its volume. Thereby, the error induced due to the effect of noise diminishes. Let,

$$\epsilon_n = u_n^v - f(u_{n-1}), \tag{31}$$

be the error due to noise. Using time delay embedding one obtains vectors of the form,

$$\varsigma_n = [\epsilon_n, \epsilon_{(n+\tau)}, \ldots, \epsilon_{(n+(D_E-1)\tau}], \tag{32}$$

In the reconstructed phase space of embedding dimension D_E, the initial separation between two nearby trajectories is denoted by, $||\varsigma_p - \varsigma_q||$ where $p \neq q$ by t_0, then we can find all pairs of vectors in phase space with their distance approximately $\leq t_0$. If we introduce a shell of radius R, then this statement amounts to,

$$R \leq ||\varsigma_p - \varsigma_q|| \leq R + \Delta R. \tag{33}$$

where $\Delta\varsigma$ is the width of the sphere and is an arbitrary chosen small distance. Then if, $\varsigma \to 0$ will indicate that the trajectories come close to each other and become comparable to each other. This, in turn implies that the error is minimized to reach the true estimate. The set of estimates for which the ML-PSV is minimum are considered to be the true estimates of the system under consideration. This is the idea behind applying ML-PSV as an objective function in parameter estimation.

Figure 2 shows the block diagram of our approach where the inverse filter reverses the system effect so that the filter output is equal to the chaotic input signal. i.e., $u_n = x_n$. By optimizing the ML-PSV objective function of the inverse filter output u_n with respect to the parameters $\hat{\mathbf{h}}$, the inverse system can identify the parameters $\mathbf{h}$ of the original system. We have applied the ML estimate of PSV in an algorithm for blind system identification of AR and MA models which is summarized in Algorithm 2:

A. CASE STUDY: APPLICATION TO BLIND IDENTIFICATION OF AUTOREGRESSIVE AND MOVING AVERAGE MODELS

Consider the following second order autoregressive (AR) model,

$$\begin{aligned} y_n &= z_n + x_n + v_n, \\ &= 0.195y_{n-1} - 0.95y_{n-2} + x_n + v_n. \end{aligned} \tag{35}$$

where $z_n = \sum_{l=1}^{L} h_l y_{n-l}$, x_n is a chaotic signal and v_n is AWGN with variance σ^2 for $n = 1, \ldots, N$. An inverse filter is employed to estimate the coefficients $\hat{h}_l$s for the AR model from the received signal y_n, that is:

$$\begin{aligned} u_n &= y_n - \sum_{l=1}^{L} \hat{h}_l y_{n-l}, \\ &= y_n - \hat{\mathbf{h}}^{\mathsf{T}} \mathbf{y}_{n-1}. \end{aligned} \tag{36}$$

Using different $\hat{h}_l$, we can get different u_n from the received signal y_n. The ML-PSV of u_n is computed and minimized by varying $\hat{\mathbf{h}} = [\hat{h}_1, \ldots, \hat{h}_L]$. Another system considered here is a second order moving average (MA) model,

$$\begin{aligned} y_n &= \sum_{l=1}^{L} h_l x_{n-l} + v_n, \\ &= x_n + 0.6x_{n-1} + 0.3x_{n-2} + v_n, \end{aligned} \tag{37}$$

where $\mathbf{h} = [h_1, h_2, \ldots, h_L]^{\mathsf{T}}$ is the channel coefficient vector with L as the order and v_n is the AWGN. The inverse filter of the MA model in (37) is given by

$$u_n = y_n - \sum_{l=1}^{L} \hat{h}_l u_{n-l}. \tag{38}$$

Algorithm 2 Algorithm for Blind System Identification Using ML-PSV

1: Given the received signal $y_n, n = 1, 2, \ldots, N$, construct an inverse system u_n where the parameter vector $\hat{\mathbf{h}}$ is the estimate of the true parameters $\mathbf{h}$.
2: Embed u_n into a D_E dimensional phase space using the delay coordinate, i.e., $\mathbf{u}_n = (u_n, u_{n+\tau}, \ldots, u_{n+(D_E-1)\tau})$ is an embedding dimension of the chaotic map $f(\cdot)$. (In this work, $\tau = 1$).
3: Calculate the ML estimate of PSV of the inverse filter output vector $\mathbf{u}_n$ using (19).
4: Minimize the ML-PSV estimate with respect to $\hat{\mathbf{h}}$, i.e.,

$$\hat{\mathbf{h}} = \arg\min_{\hat{\mathbf{h}}}(\hat{V}_{ML}(\hat{\mathbf{h}})) \tag{34}$$

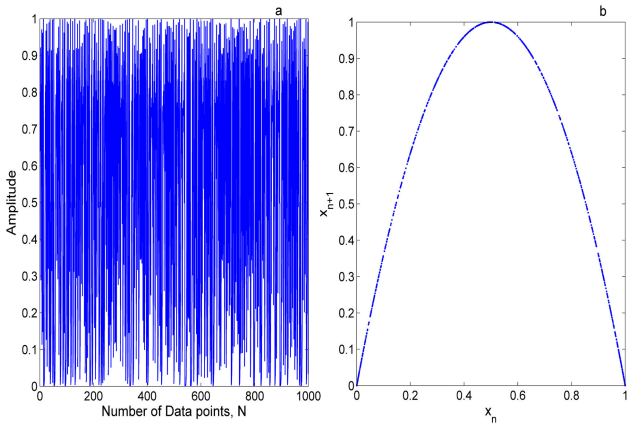

FIGURE 3. (a) The transmitted chaotic data (b) Phase space plot of the chaotic Logistic map.

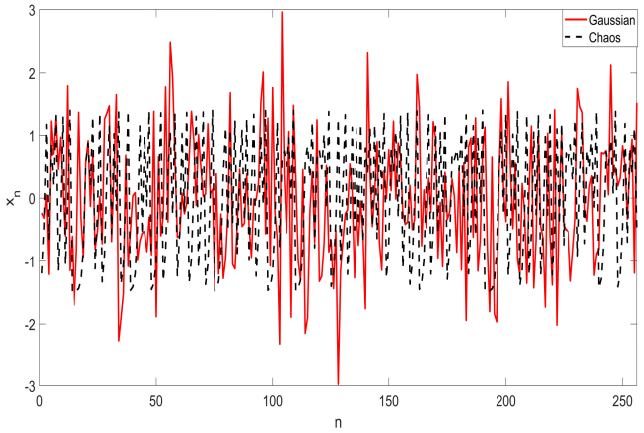

FIGURE 4. Typical waveform of white Gaussian and chaotic signals.

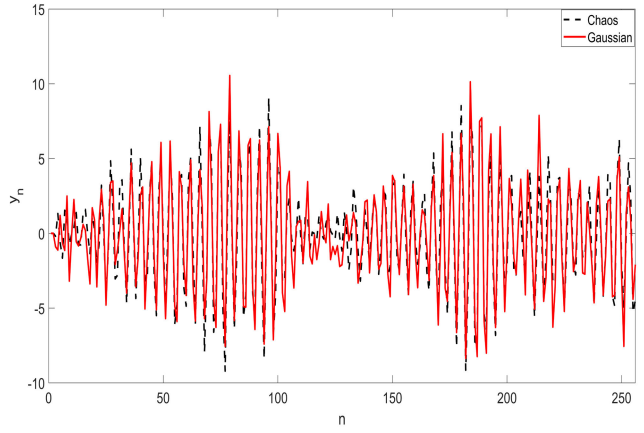

FIGURE 5. Signal waveforms of the noise-free AR system output: $y_n = 0.195y_{n-1} - 0.95y_{n-2} + x_n$ driven by the logistic map chaotic signal x_n and a Gaussian signal.

However, only y_n is known in the above equation and $\hat{\mathbf{h}}$ is the unknown parameter vector that is to be estimated. A zero mean and unity variance chaotic signal x_n is generated by the chaotic logistic map:

$$x_n = \gamma x_{n-1}(1 - x_{n-1}). \tag{39}$$

The logistic map exhibits chaotic phenomenon if the parameter γ falls in the range $(3.56995, 4]$ with x resembling white noise. When the system is chaotic, its time series output is an ergodic process and can be considered as white noise according to the correlation property. Figure 3 shows the time series obtained from the chaotic logistic map along with its phase space plot where $\gamma = 3.98$. Since x_n is white, for the purpose of system identification comparison we considered two kinds of driving signals: zero-mean WGN process with unit variance and a zero-mean chaotic signal with unit variance generated by the chaotic logistic map in (39). Figure 4 presents the chaotic and random input sequence and Figure 5 and Figure 6 shows the corresponding outputs of the AR and MA models using the chaotic and Gaussian signals. The SNR range used throughout this work unless otherwise stated is $0 : 5 : 40$ dB.

In the absence of noise, the ML-PSV obtained for the AR(2) and MA(2) is 0.7351 known as the true ML-PSV volume using $N = 256$ data points with one trail for $D_E = 2$ and $\tau = 1$. The performance of blind system identification is expressed in terms of MSE between the desired $\mathbf{h}$ and the estimated parameters of the system $\hat{\mathbf{h}}$ as,

$$\text{MSE}_h = \frac{1}{K}\frac{\sum_{i=1}^{K} ||\mathbf{h}_i - \hat{\mathbf{h}}_i||^2}{L} \tag{40}$$

In (41) K is the number of independent trials. The results in the following sections are obtained by considering the $r_1 = 0.5$ and $r_2 = 1$, $m = 1$ and embedding dimension, $D_E = 2$. In this work, $r_1 = 0.5$ gave the minimum MSE_h performance for both the AR and MA models followed by $r_2 = 1$ as shown in Figure 7. It shows the MSE_h performance for AR(2) model

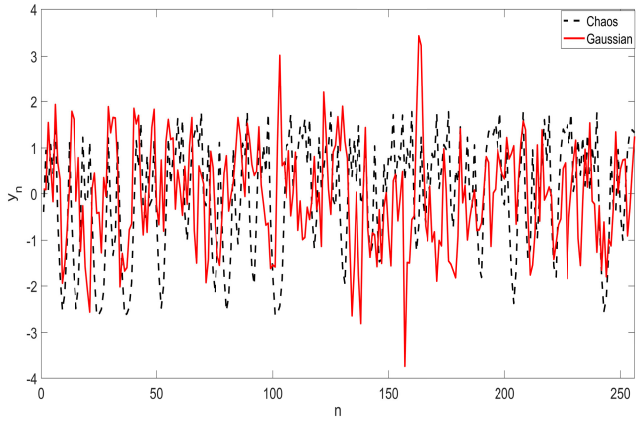

FIGURE 6. Signal waveforms of the MA system output: $y_n = x_n + 0.6x_{n-1} + 0.3x_{n-2}$ when x_n is generated from a logistic chaotic map and Gaussian signal respectively.

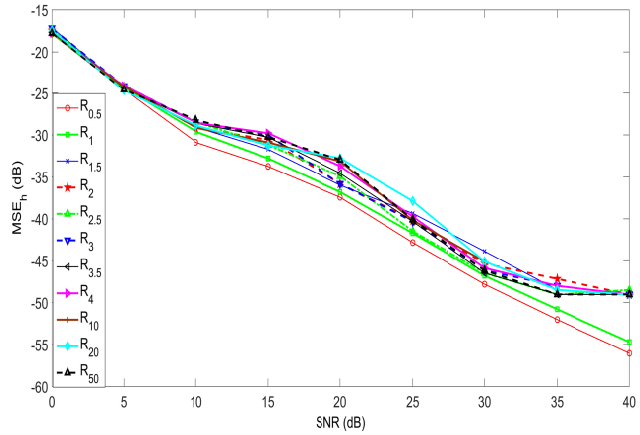

FIGURE 7. Effect of radius on blind system identification performance for AR model.

plotted for each radius using $N = 256$ and $K = 30$ trials. We have used $K = 30$ since the variance of MSE_h is reduced to a relatively small value after that. The MSE_h obtained with $r_1 = 0.5$ and $r_2 = 1$ gives the best performance at a low SNR of 0dB and high SNR of 40 dB. We observed a similar trend for the MA model.

B. PERFORMANCE EVALUATION IN ABSENCE OF NOISE

A typical identification example for one trial is reported in Table 1 which shows the performance of the MPSV and ML-PSV methods in blind system identification of the AR and MA systems in the absence of noise for $K = 1$ trial. In the absence of noise, the volume of the phase space is invariant of the density of the data points, $p(\cdot)$ when the number of points are constant [52]. Thus, the ML-PSV estimate and the PSV of the original method (MPSV) does not change during the parameter estimation of the AR and MA models. The distance between pairs of points remains the same in the absence of noise. However, this imposition does not hold true in the case of noise corrupted time series which causes the data points in the phase space to get dispersed thereby increasing the value

TABLE 1. Blind system identification performance of AR (2) and MA(2) models using MPSV and ML-PSV for noise free case and K = 1.

Model	MSE	$\hat{h_1}$	$\hat{h_2}$	MPSV
AR	7.7037 e-33	0.1950	-0.9500	6.2490
MA	1.2500 e-05	0.6000	0.3000	6.9926

Model	MSE	$\hat{h_1}$	$\hat{h_2}$	ML-PSV
AR	7.7037e-33	0.19000	- 0.9500	0.7351
MA	1.2499e-05	0.6000	0.3000	0.7351

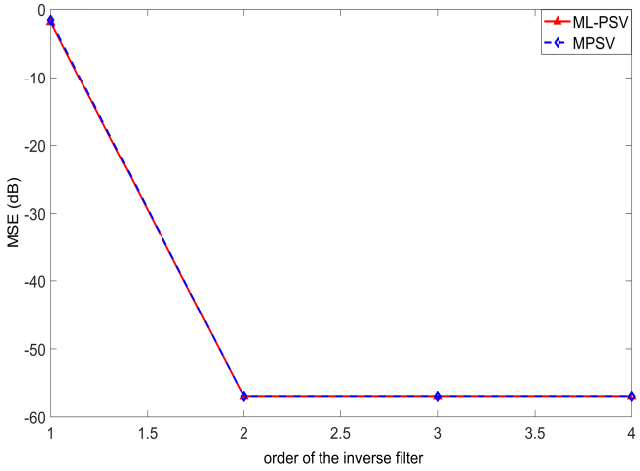

FIGURE 8. Effect of inverse filter order on MSE of the estimated coefficients of AR model.

of PSV. Thus, the PSV and the ML-PSV values vary with SNR. From Table 1 it can be inferred that both the techniques perform equally well in the absence of noise.

1) EFFECT OF ORDER OF INVERSE FILTER ON ESTIMATION

Figure 8 presents the results obtained by varying the order of the inverse filter only without changing the order of the considered AR model. MSE_h, the PSV and the ML-PSV estimate remained about the same level for order ≥ 2. Similar result was obtained for the MA(2) model. This shows that for both the techniques an order determination is not required.

2) EFFECT OF NUMBER OF DATA POINTS

To study the effect of data length N on the system identification performance using MPSV and ML-PSV identification techniques, MSE_h of the AR(2) is plotted against different number of data points for $K = 1$ trial in Figure 9. It can be seen that the error depends on N and identification performance improves with the increase in length of the signal. However, this leads to the increase in the computational load. Figure 10 shows the effect of the number of data points on the value of PSV calculated from the MPSV method and the proposed ML version. It is observed that PSV increases with the increase N. This result is intuitive since the derived ML-PSV estimate of the PSV directly depends on the number of points inside a bounded region and as such the PSV of the chaotic system will depend on the number of the data points. Similar trend is observed for the PSV of the original

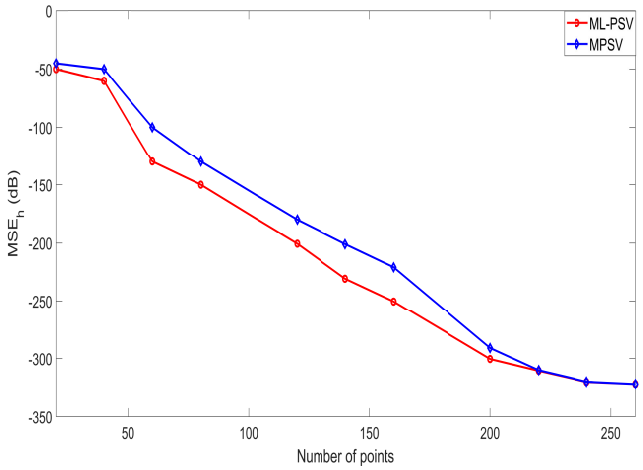

FIGURE 9. Effect of length of chaotic numeric signal on system identification using MPSV and ML-PSV.

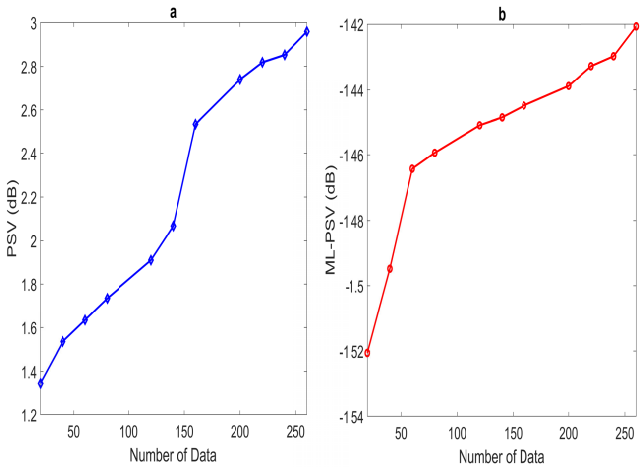

FIGURE 10. Effect of length of chaotic numeric signal on PSV using MPSV and ML-PSV for the (a) AR(2) and (b) MA(2) models.

MPSV method. It can also be concluded that the proposed ML estimate of the PSV yields a smaller PSV value in contrast to MPSV. Similar observations were observed for the MA model.

C. PERFORMANCE IN AWGN USING CHAOTIC NUMERIC SIGNAL

Blind system identification performance comparison is shown in Figure 11 and Figure 12 for AR(2) and MA(2) models respectively. The proposed blind ML-PSV is compared with blind MPSV, EM-UKS [32], MNPE, nonblind LS with chaos and nonblind LS with WGN at various SNR levels of AWGN of zero-mean and variance 1. Since x_n is $i.i.d.$ and non-Gaussian, blind system identification performance of ML-PSV is compared with HOS based blind methods such as the CUM3 and CUM4. After equalization with CUM3 and CUM4, least mean squares (LMS) is applied to obtain the estimates of the AR and MA models. ML-PSV is found to outperform the HOS methods at all levels of SNR. The difference between ML-PSV and MNPE identification

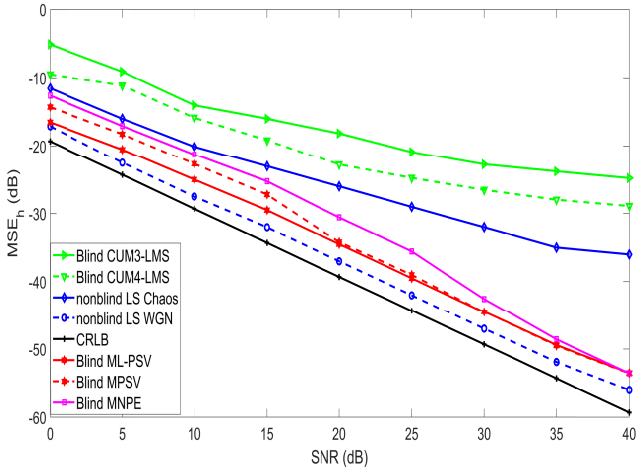

FIGURE 11. Blind Identification performance of AR model in AWGN.

methods is that the MNPE method estimates the system coefficients by minimizing the prediction error of the inverse filter output. On the other hand, our method uses the ML estimate of the dynamic metric of chaotic signals known as the PSV. The ML-PSV estimate is applied to the output of the inverse filter, minimize of the parameters of the inverse filter expects to yield the true parameters of the original system. The authors in [25] proved that using a WGN as the driving signal, the nonblind identification with LS is shown to achieve similar performance to blind identification with chaos. Furthermore, using chaos the nonblind identification performance with LS is poor than the blind identification using chaos. In that work, it was also proved that the CRLBs of nonblind identification using WGN is equivalent to that of blind identification when a chaos driving signal is used. Therefore, MPSV and ML-PSV methods perform quite similar to the nonblind LS method with WGN but outperforms the nonblind LS with chaos. In addition, our results show that the proposed ML-PSV and the existing MPSV method is robust as all extra coefficients for the AR(2) and MA(2) models are very close to zero. For the LS method, however, these coefficients still take a relatively large value. An order determination method has to be used with the LS method to determine if some coefficients are extra. Since the LS method obtains minimal mean square error between the estimated parameters and true parameters when the driving signal is Gaussian, it implies that the performance of the LS identification method degrades when the driving signal is non-Gaussian. Therefore, it is a good choice for performance comparison to use the statistically optimal LS method when the driving signal is a zero-mean WGN. Hence, when x_n is a WGN process, the standard nonblind LS method is employed for performance comparison.

1) PERFORMANCE EVALUATION FOR AR MODEL USING CHAOTIC NUMERIC SIGNAL IN AWGN

In Figure 11, the MSE_h performance of blind system identification using chaotic numeric (CN) signal for AR(2) model

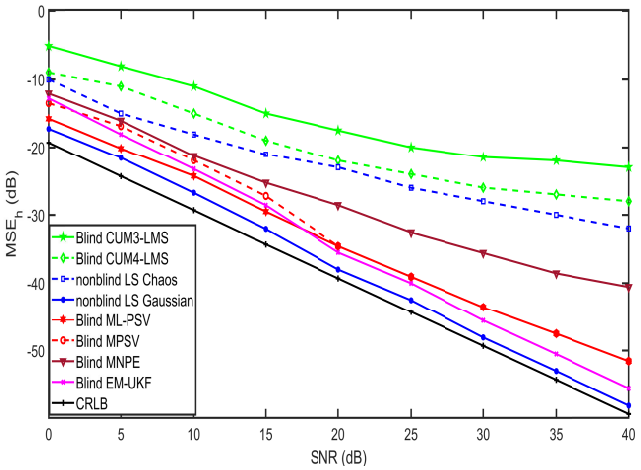

FIGURE 12. Blind Identification performance of MA model in AWGN.

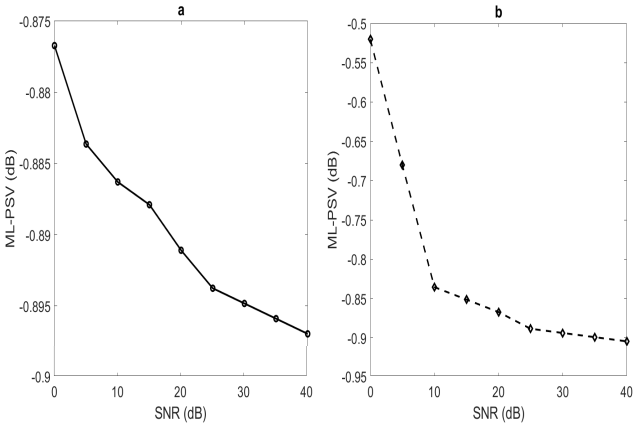

FIGURE 13. Variation of ML estimate of PSV with SNR in blind system identification of (a) AR(2), and (b) MA(2) models for K = 30 trials.

is shown with $N = 256$ data points and $K = 30$ trials. For both the AR and MA models, ML-PSV method provides an improvement of 2.3 dB at 0-15 dB SNR in comparison to the existing MPSV in presence of AWGN. However, at SNR >= 20 dB both the methods yield similar performance. Therefore, the proposed ML-PSV definitely shows an improved performance of about 2.3 dB over MPSV at low SNR for both the AR(2) and MA(2) models. ML-PSV shows a significant improvement over nonblind LS with CN driving signal at high SNR. This is because the LS method is suboptimal for non-Gaussian signal such as the chaotic signal and at high SNR chaos dominates the Gaussian signal. This result further reinstates our claim that the application of a chaos-based estimator such as the proposed ML-PSV aids in parameter estimation when using chaotic signals since the estimator encapsulates the properties/information of the chaotic signal. Furthermore, ML-PSV also outperforms the blind MNPE and HOS methods at all levels of SNR. The blind MNPE method shows performance comparable to that of ML-PSV and MPSV only at SNR > 25 dB. ML-PSV lacks behind nonblind LS with WGN by about 1.5 dB at 0 dB SNR. However, it can also be observed from Figure 11 that ML-PSV lacks behind the nonblind LS with WGN by about 2 dB SNR and lacks behind the CRLB by approximately 5 dB SNR all throughout. Both the ML-PSV and MPSV methods do not reach the CRLB performance and give poor performance in comparison to the statistically optimal LS method. In order to improve the performance of ML-PSV with chaos, we propose to apply symbolic dynamics to convert the chaotic numeric signal to chaotic symbolic (CS) signal. This is explained subsequently.

2) PERFORMANCE EVALUATION FOR MA MODEL USING CHAOTIC NUMERIC SIGNAL IN AWGN

Figure 12 shows the nonblind identification with LS with chaos is no longer optimal and its performance is worse than that of nonblind LS with WGN. In comparison to the EM-UKF with chaos, ML-PSV shows a significant performance improvement of about 3 dB at 0 dB SNR. From 5-15 dB SNR, ML-PSV approach closely follows the EM-UKF thereafter ML-PSV performance degrades. ML-PSV lacks behind nonblind LS with WGN by about 1.5 dB at 0 dB SNR, similar to that of the AR model. Once again, as SNR increases both ML-PSV and MPSV methods perform similarly.

Figure 13 illustrates that as the SNR increases, the ML estimate of the PSV gradually decreases for AR and MA models respectively. As observed, the ML-PSV and its CRLB has a monotonic decreasing trend with the increase in SNR in Figure 14 which is for the MA model (since similar trend was observed for the AR model), as is the case for the MSE_h in Figures 11 and 12. Figure 14 shows the plot of the MSE of the ML-PSV estimate for the MA(2) model and the CRLB of the ML-PSV estimate. The MSE was calculated between the true ML-PSV under noise-less condition and the ML-PSV at various SNRs and averaged over K = 30 trials when the AR and MA models are corrupted by AWGN at SNR = 0 : 5 : 30 dB. It is observed that the MSE of the ML-PSV estimated for the AR model gradually approaches the CRLB of the ML-PSV estimate. This result shows that as noise reduces, the ML-PSV estimate of the inverse filter output gradually reaches the minimum which should be close to that of the true estimate of ML-PSV in the absence of noise and this value corresponds to the true parameters of the MA(2) model as shown in Figure 13(b).

3) EFFECT OF HIGHER DIMENSION ON ESTIMATION PERFORMANCE USING CHAOTIC NUMERIC SIGNAL

Here we examine the MSE_h performance with respect to the embedding dimension, D_E for the MA model with chaotic numeric input at SNR = 15 dB. On each trial, the embedding dimension is held constant and the MSE_h is plotted versus different embedding dimensions in Figure 15 for $K = 30$ using $N = 256$ data points in each trial. It is observed that the minimum MSE_h of approximately -25 dB occurs when the embedding dimension $D_E = 2$ for the chaotic Logistic map that has an attractor dimension (intrinsic dimension) of

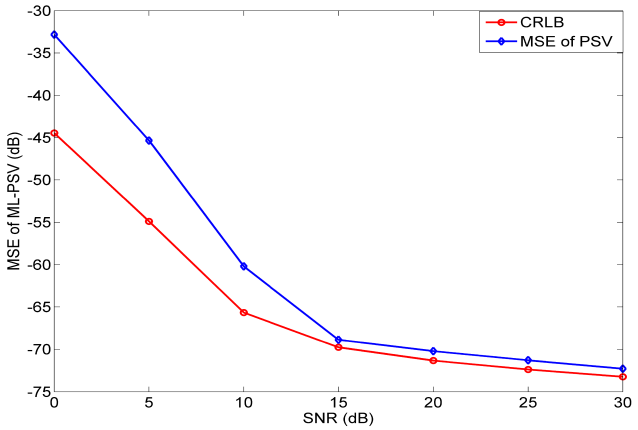

FIGURE 14. CRLB of the estimate of ML estimate of PSV and the MSE of these estimates using the PSV of the Logistic map.

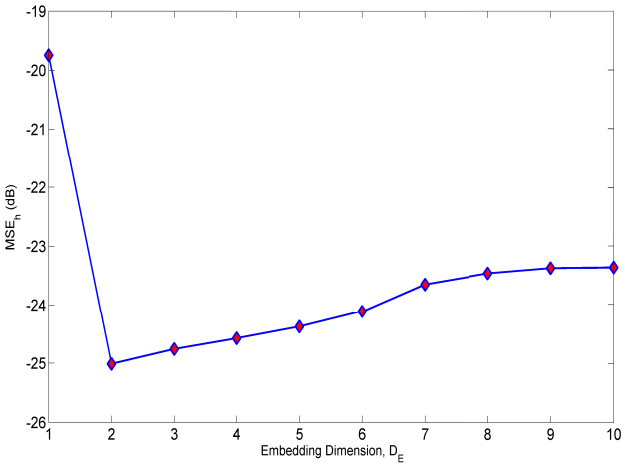

FIGURE 15. Effect of embedding dimension on MSE of estimated parameters of the MA model at SNR = 15 dB.

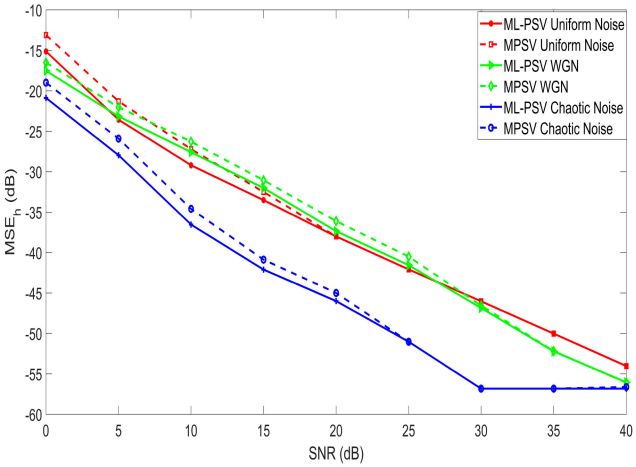

FIGURE 16. Comparison of blind system identification for AR(2) in WGN, Uniform and chaotic noise using CN signal.

$m = 1$. This is due to the reason that with the knowledge of the attractor dimension m used for generating a chaotic signal, the ML-PSV can be minimized by adjusting the parameters of the inversely filtered signal by using Whitney's minimum Embedding theorem using an embedding dimension of $D_E >= 2m$ [51]. Since the chaotic logistic map is a 1-D dynamic, an embedding dimension of two should be sufficient for phase-space reconstruction. As a result, the MSE_h performance drops from $D_E = 1$ to 2 and stays at the same level for any higher embedding dimension. Although the MSE drops from $D_E = 1$ to 2 as expected, it increases steadily for higher embedding dimensions. The reason is that the ML-PSV calculation depends on the number of points. For $D_E = 2$, $N = 256$ points are enough to display the dynamics of the signal. However, for higher embedding dimensions like $D_E = 4$, 256 points are dispersed in the 4-D phase-space and distributed scarcely. In fact, it has been shown before that for a chaotic signal it is expected that the error will decrease to an optimal value as the embedding dimension is increased to the correct minimal embedding dimension, and remains close to the minimum error level when the dimension exceeds the minimal embedding dimension. The result from Figure 15 supports our choice of selecting the embedding dimension as $D_E = 2$. For the AR(2) model, similar observation has been noted.

D. NOISE SENSITIVITY ANALYSIS

The evaluation of blind system identification performance under different kinds of measurement noise is presented for AR(2) and MA(2) models in Figure 16 and Figure 17 respectively. The blind identification performance of ML-PSV is compared with blind MPSV using CN signal for different kinds of measurement noise, v: (a) WGN of a fixed variance of 0.5, (b) Uniform White noise, and (c) chaotic noise using $N = 256$ data points and $K = 30$ trials. From Figure 16 it is observed that when the AR(2) model is corrupted by WGN noise of variance = 0.5, ML-PSV method shows an improvement of approximately 1dB over MPSV at SNR = $0 - 25$ dB after which both the methods show quite similar performance. However, when the received signal is corrupted with a Uniform White noise, ML-PSV method shows an improvement of 2 dB for SNR = $0 - 10$ dB over MPSV. Gradually from SNR >= 15 *dB* onwards, both the techniques show same performance. Figure 16 also shows the MSE_h performance from measurements corrupted by a chaotic signal that is obtained from another chaotic map known as the Tent map. It is a one dimensional chaotic dynamical system in the unit interval [0, 1] and is represented by the following dynamical system:

$$g : [0, 1] \rightarrow [0, 1]$$
$$g(v) = \begin{cases} 2v, & \text{for } 0 \leq v \leq 1/2 \\ 2 - 2v, & \text{for } 1/2 \leq v \leq 1 \end{cases} \quad (41)$$

Iterating the chaotic Tent map in (41) generates a time series $(v_0, v_1, v_2, \ldots, v_n, \ldots, v_{N-1})$ where each v_n is a point in the unit interval [0, 1]. ML-PSV shows a performance improvement of approximately by about 5-6 dB at 0 dB and 5 dB

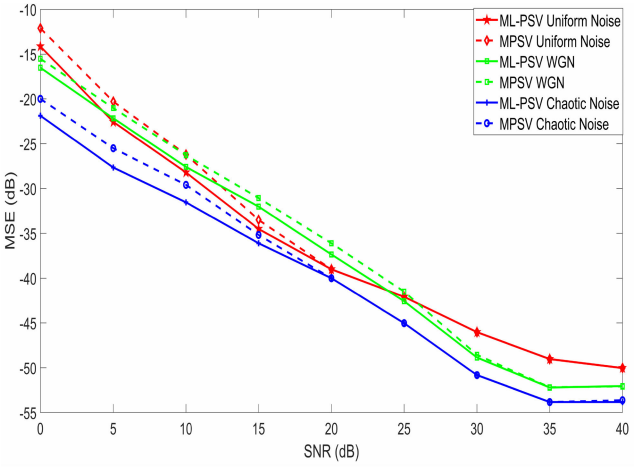

FIGURE 17. Comparison of blind system identification for MA(2) in WGN, Uniform and chaotic noise for CN signal.

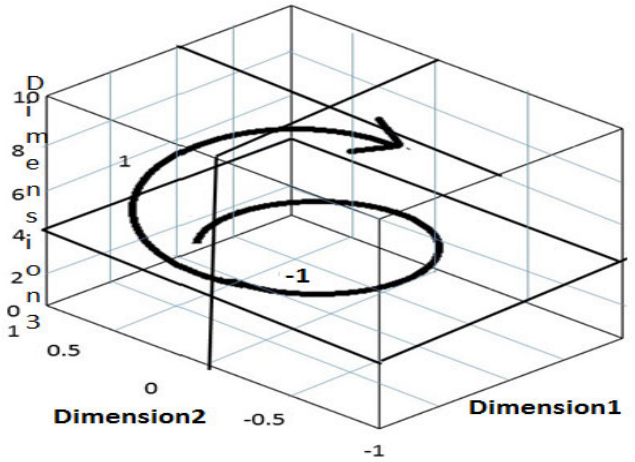

FIGURE 18. Illustration of the evolution of time series in phase space and associated symbols.

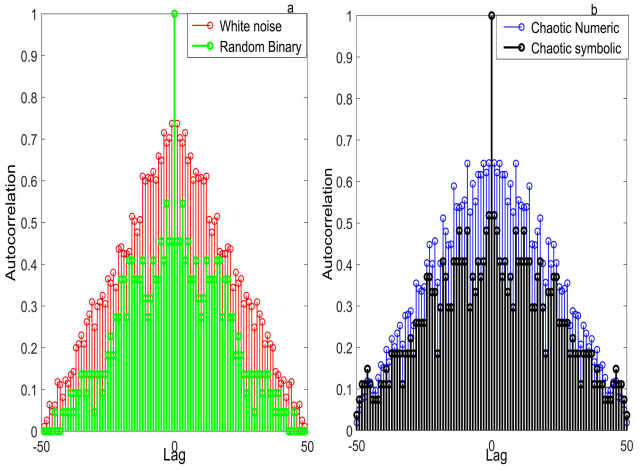

FIGURE 19. Normalized auto-correlation function (a) Random signal (b) Chaotic signal.

SNR in comparison to being corrupted with AWGN. Thereafter, the performance of ML-PSV under the influence of chaotic measurement noise increases by 11 dB to 12 dB for SNR = [10,15,20,30] dB. In comparison to MPSV, ML-PSV achieves a performance improvement of 2 dB at SNR = 0-10 dB. Eventually, both the methods perform similarly giving the lowest MSE_h performance amongst all kinds of noises. This is because the addition of chaotic signal fills the phase space with data points from chaotic systems and as such the dynamic estimators are able to capture more information from the chaotic dynamics. The blind identification performance of the proposed ML-PSV method shown in Figure 17 for the MA(2) model shows similar performance improvement in chaotic noise. From these results, we can infer that blind system identification of AR and MA models with ML-PSV and MPSV methods are most resilient to distortion from chaotic noise and ML-PSV gives superior performance over MPSV method overall. ML-PSV gives the worst performance for measurements corrupted by AWGN.

E. BLIND SYSTEM IDENTIFICATION WITH CHAOTIC SYMBOLIC SIGNAL

The choice of driving input signals has an important role in system identification. Here we discuss the advantage of using CS over CN in improving system identification performance using chaos. The results obtained reinstates the rationale for selecting a CS signal as a candidate for driving input signal in system identification. A symbolic time series signal generated by a chaotic system by the method of symbolic dynamics is denoted as a chaotic symbolic (CS) signal. Symbolic dynamics is a method that converts the real-valued trajectories into symbol sequences. This method helps to study the dynamics of the chaotic system using symbolic representation. In essence we divide the phase space of the system, assign a symbol to each section of the phase space, and create a symbolic sequence by looking at the time series that passes through these divisions. Pictorically, the concept of symbolic dynamics is illustrated in Figure 18 for an embedding dimension $D_E = 3$. The phase space is partitioned into two regions, each of which is labelled with a unique symbol ± 1 according to a rule. Each data point (state) in the phase space gives a sequence of symbols and the evolution of the system is described by the progression of these symbols. In general, we can consider only one variable to obtain the symbolic dynamics. In this work, a symbolic sequence is generated by a chaotic map as:

$$s_n = \begin{cases} +1, & \text{if } x_n \geq \mu \\ -1, & \text{otherwise} \end{cases} \tag{42}$$

where $\mu = \frac{1}{N}\sum_{n=1}^{N} x_n$ is the mean of the chaotic signal.

It is desirable to analyze the properties of the CN and CS signals as well as random binary signal known as pseudo-random binary signal (PRBS). We study the average cross correlation function and the crest factor which are the properties of a signal required for system identification. The average cross correlation function of CN and CS signals are shown in Figure 19. From Figure 19(a) and 19(b) it can be observed that the auto-correlation of a random binary

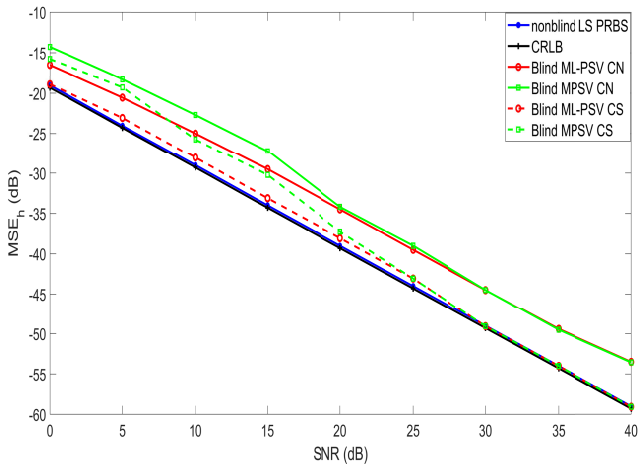

FIGURE 20. Performance comparison using CN and CS signals in system identification of the AR(2) model in AWGN.

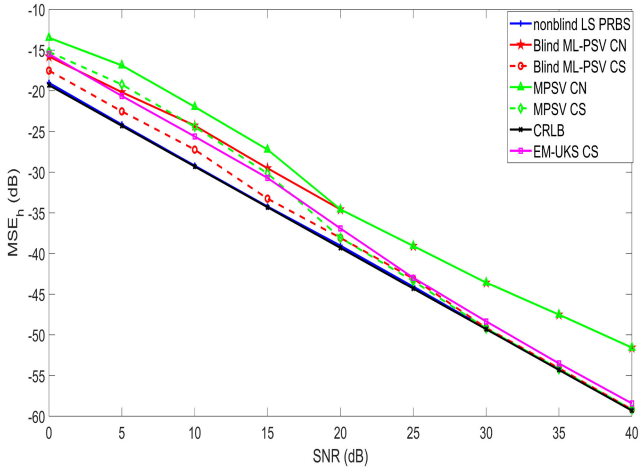

FIGURE 21. Performance comparison using CN and CS signals in system identification of the MA(2) model in AWGN.

signal and the CS signal are similar to each other having a pure delta function. A signal having a pure delta function means that it only correlates with itself at lag = 0. Therefore, closer the auto-correlation of a process is to a delta function, it is more uncorrelated. This is a desirable property since it means that the signal achieves the largest power having a maximum amplitude. In other words,the CS has better frequency spectrum suitable for system identification compared to the numerical sequence. Figure 19(b) clearly shows that for a finite chaotic sequence, the correlation function of the CS signal has better peak to valley ratio compared to its numerical counterpart. This implies that the CS has even have better frequency spectra for system identification. Another guideline for choosing the input signal is that it should be able to deliver as much input power to the system as possible. The smaller the crest factor, the better the signal excitation. A better signal excitation results in larger total energy delivery and enhanced signal-to-noise ratio. The theoretical lower bound for the crest factor is 1. From numerical simulations, the crest factor for the CN signal obtained is 1.9901 dB and 1.4468 dB for CS signal. Thus, the CS sequence transfers more energy to the system which results in a better system identification performance. These properties of chaos helps in system identification where the CS acts as the driving signal. As a result, a CS obtained from a CN can play an important role in our work.

We now present results demonstrating the advantage of using CS over CN in improving system identification performance. Figures 20 and 21 demonstrate the effectiveness of using a CS over CN in driving the models for blind system identification which are obtained using $N = 256$ and $K = 30$ trials. When x_n is generated from a random general signal which is a zero mean white Gaussian process with unity variance, we have applied the LS technique. In Figure 20 for the AR(2) model, the MSE_h performance using the ML-PSV method with the CS signal shows a performance improvement of 2.4 dB over its CN counterpart at 0 dB SNR which gradually improves giving an improvement of 5 dB at SNR = 40 dB. Similar performance improvement is obtained by ML-PSV using CS for the MA(2) model as observed from Figure 21. The impact of using CS over CN signals is that the CS signal helps the MSE_h performance for both the methods to reach the performance of the nonblind LS with PRBS which otherwise showed poor performance with CN signal before. ML-PSV with CS shows improved performance over CN signal in comparison to EM-UKS with CS. At 0 dB SNR, ML-PSV with CS signal shows a performance improvement of about 2 dB in comparison to EM-UKF with CS. The performance improvement by ML-PSV with CS over EM-UKS with CS continues from $5 - 15$ dB and thereafter both show similar performance. On the other hand, ML-PSV with CS shows better performance at $0 - 20$ dB SNR in comparison to MPSV with CS. The proposed ML-PSV estimation technique with CS input lacks behind nonblind LS with PRBS by about 1.5 dB at 0 dB SNR and then by 1 dB for SNR $= 0 - 25$ dB giving similar performance thereafter.

V. EXPERIMENTAL EVALUATION

In this section we evaluate the performance of the dynamic based identification method through experimental evaluation using software defined radio (SDR) for blind equalization in wireless communications for which ARMA model is seldom used. An AR model considered as an autoregressive moving average (ARMA) should be able to be approximated by an AR with sufficient order. The experimental results validate the improved equalization performance of the proposed ML-PSV method. In this work, we have applied our ML-PSV estimate for equalization of a fading and multipath channel that is modeled by an FIR filter. Thus, the received signal is represented as:

$$y_n = \sum_{l=1}^{L} h_l x_{n-l} + v_n. \tag{43}$$

where $\mathbf{h} = [h_1, h_2, \ldots, h_L]^{\mathsf{T}}$ is the channel coefficient vector with L as the order and v_n is the AWGN with variance σ^2. The objective of blind identification/equalization is to estimate the

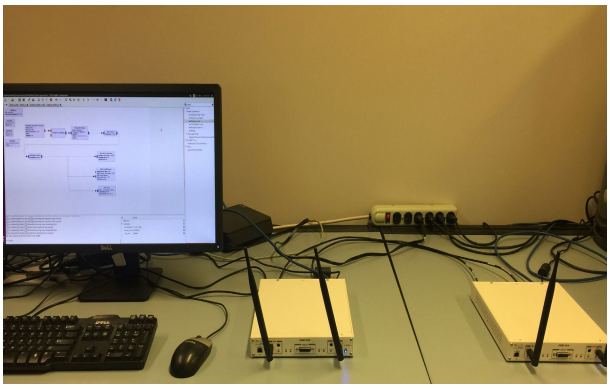

FIGURE 22. Experiment environment.

unknown channel parameters $\mathbf{h}$ and the transmitted chaotic signal x_n from the received noisy signal y_n. We apply the ML-PSV estimator derived in (19) as the objective function in (34) for blind system identification using noisy observations y_n only. The inverse filter of (43) is given by,

$$u_n = y_n - \sum_{l=1}^{L} \hat{h}_l u_{n-l}. \tag{44}$$

However, only y_n is known in the above equation and $\hat{\mathbf{h}}$ is the unknown parameter vector that is to be estimated.

A. EXPERIMENTAL SETUP

The purpose of the experiments is to generate chaotic signals using software and passing it through a system model to demonstrate the merit of ML-PSV estimator in blind equalization. The experiment setup for blind equalization is demonstrated in Figure 22. It includes two Universal Software Radio peripherals (USRP), each controlled by a desktop computer via an Ethernet cable. The USRP is a SDR platform equipped with a X310 motherboard, a WBX-120 daughterboard that covers 50 MHz to 2.2 GHz frequency band, and two omnidirectional antennas. The softwares installed on the desktop, including USRP Hardware Driver (UHD) and GNURadio, allow users to control and communicate with USRP devices. Then we use one USRP to transmit it on radio frequency (RF), and use the other one as a receiver. At the transmitter side, a self-defined module generates a sequence using the logistic map in (39) with initial condition $x_0 = 0.8$. Without loss of generality, we choose $\gamma = 3.98$. The generated sequence is shown in Figure 23. The chaotic signal then passes through a MA(2) model or an FIR system with impulse response $\mathbf{h} = [1, 0.6, 0.3]^{\mathsf{T}}$. Note that the chaotic signal we get has a mean value of 0.5518. The actual values of the MA coefficients are assumed to be known for the purpose of MSE calculation. These values are unavailable at the receiver. After passing the chaotic signal through the FIR system, the signal contains a non-zero DC component and its maximum amplitude exceeds 1. As we cannot transmit DC component over RF and the USRP does not allow amplitude greater than 1, we remove the DC component by

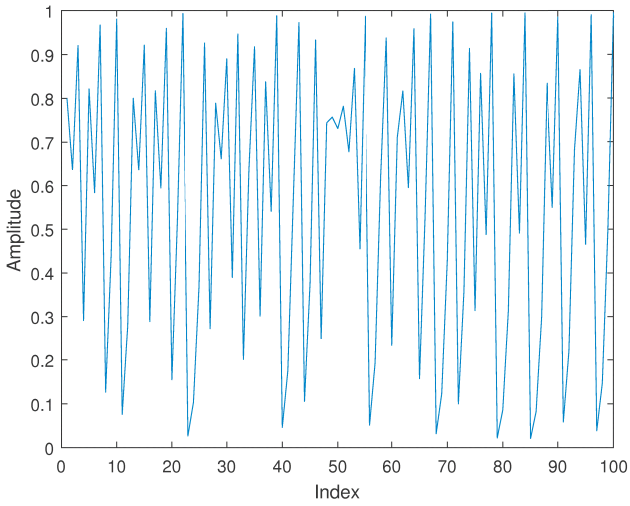

FIGURE 23. Logistic map time domain signal.

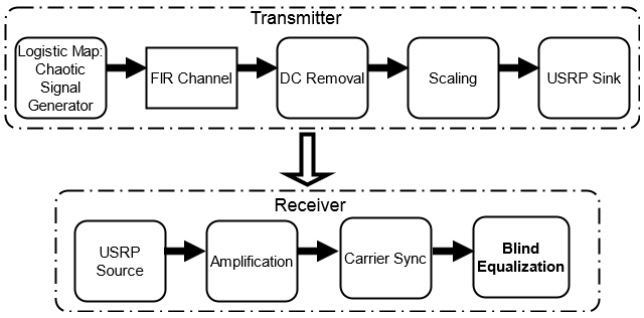

FIGURE 24. Schematic diagram of the transmitter and receiver design in GNURadio.

subtracting the mean value and scale down the signal. After that, the USRP transmits the signal at a speed of 2 M Samples/s on the 915 MHz ISM band.

Figure 24 shows the schematic diagram for the transmitter and receiver. The USRPs have independent clocks. If they are not synchronized, the received signal would be different from the transmitted one. Hence we use one clock to provide reference signals through the hardware port to the other one so that the timing error is minimized. We also amplify the received signal. It does not change the chaotic nature and has no impact on system identification performance. Although we transmit a real signal, the received one is complex due to the channel delay. We use a Costas loop to perform carrier synchronization so that the phase rotation is corrected. The two SDRs are placed relatively close to each other so that the channel noise can be considered as AWGN. At the end, we perform blind equalization using the received signal.

B. EXPERIMENT RESULTS

MSE_h is used as the performance measure to evaluate the system identification performance in AWGN for $N = 1000$ and $K = 30$ and use the real component of the received signal from experimental setup. Figure 25 shows the result of the comparison of blind system identification under the experimental setup. The simulation result of the ML-PSV

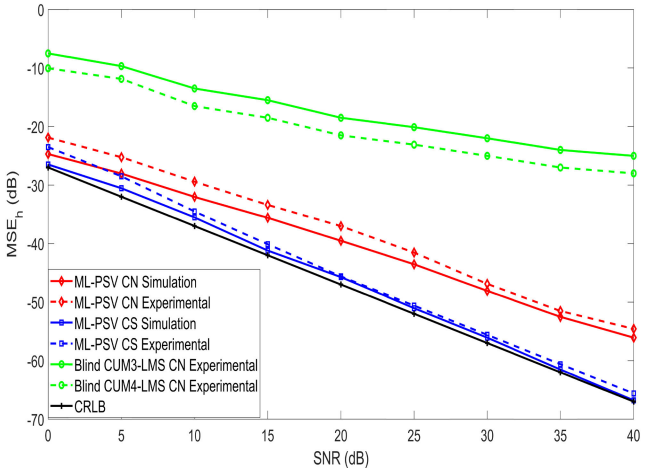

FIGURE 25. Comparison of simulation and experimental MSE_h performance of ML-PSV for MA model using CN and CS signals.

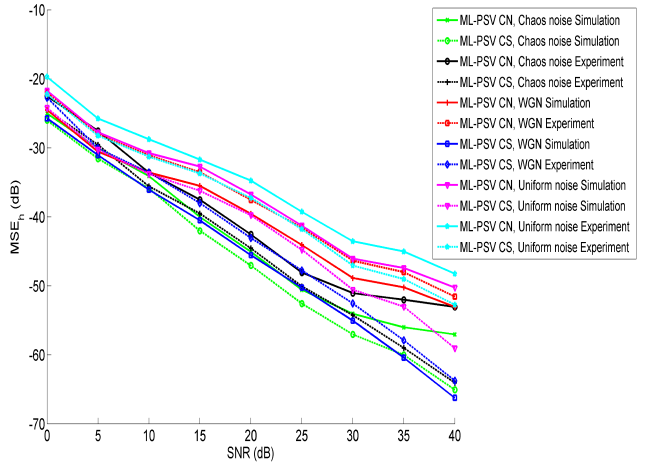

FIGURE 26. Comparison of simulation and experimental MSE_h performance of ML-PSV using CN and CS signals corrupted by different types of measurement noise.

method lacks behind its experimental result using CN by about 2.8 dB at SNR = 0−15 dB. Thereafter, the performance gap reduces to 1.5 dB. However, the experimental result of ML-PSV using CS shows remarkable improvement lacking behind its simulation counterpart by less than 1 dB SNR. Both simulation and experimental results gradually reach the CRLB performance with CS signal. Thus, once again the experimental results show the merit of using CS signal in system identification. In contrast, the HOS methods show poor performance all throughout.

In Figure 26, the blind identification performance for experimental and simulation is compared for the FIR channel corrupted by different types of measurement noise. It can be seen that the blind identification performance of ML-PSV under chaotic measurement noise gives the best MSE_h performance followed by WGN with fixed variance and the worst performance is given by Uniform noise for both the CN and CS types of signals. Once again, it is observed that eventhough the ML-PSV with CN signal performs poorly for different cases of noise, the CS counterpart boosts its

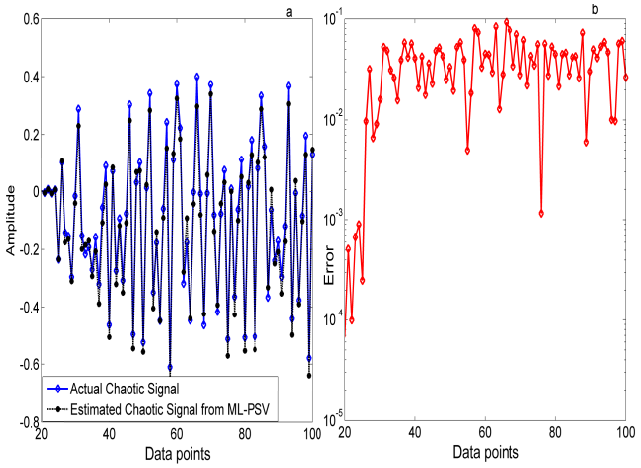

FIGURE 27. Equalization performance for MA model using ML-PSV with CN signal at SNR = 15 dB.

performance by a huge margin. Figure 27 shows the equalization result for the AWGN measurement case using CN plotted for the first 100 data points. The equalized signal is the estimated chaotic numeric valued signal which is obtained from deconvolution of the received noisy signal at SNR = 15 dB using ML-PSV method. The equalized signal that is plotted in Figure 27(a) closely resembles to the actual known chaotic signal with its error plot in Figure 27(b) remaining near zero. Therefore, the performance of the proposed ML-PSV method is validated using experiments to show improved performance over blind HOS based methods using CN signal.

VI. CONCLUSION AND DISCUSSION

The objective of this work is to derive a parameter estimation method for improving blind system identification performance when the input driving signal is an unknown chaotic signal. The motivation for using chaos as the driving input signal is based on previous research findings where it has been proved that chaotic signals are effective in system identification. One such method which applies chaotic signal for blind identification is the MPSV method. However, it has been found that it does not perform well at high noise level. To tackle this problem, we present a new improved method of MPSV technique. Our proposed method is based on deriving the PSV estimate using maximum likelihood formulation. The derived ML estimate of PSV is denoted as ML-PSV. We have also derived the CRLB of the PSV estimate and shown that the the mean square error of the PSV gradually approaches its CRLB.

We then applied the derived ML estimate of PSV (known as ML-PSV) in an algorithm as an objective function for blind system identification of AR and MA models, minimizing it with respect to the inverse filter coefficients we expect the inverse filter coefficients to get close to the true system parameters. Our results show that the proposed new method is an improved version of an existing method known as the Minimum Phase Space Volume (MPSV). ML-PSV method provides an improvement of 2.3 dB at 0 − 15 dB SNR in

comparison to the existing MPSV in presence of AWGN. At SNR >= 20 dB both the methods yield similar performance. The performance of the proposed method is compared with CRLB of WGN and nonblind LS. By comparing to the conventional blind identification methods based on higher order statistics (HOS) and chaos-based methods, the proposed ML-PSV based blind identification was shown to have superior performance at low SNR region of 0 : 5 : 15 dB. Noise sensitivity analysis shows that ML-PSV method yields the best performance for measurements corrupted by chaotic noise.

We have also evaluated the performance of our approach in blind system identification using chaotic symbolic CS) signal obtained from the symbolic dynamics of the chaotic numeric (CN) valued signal. Our results showed that the performance of CS signal using ML-PSV is better than that of CN signal for both the AR(2) and MA(2) models. ML-PSV method with CS achieves performance close to nonblind with PRBS. Furthermore, with CS the ML-PSV method showed improved performance at SNR = 0 : 5 : 20 dB in comparison to EM-UKF with CS thereafter both the methods yielded similar performance. It can be observed that the MSE_h of the proposed method with CS closely follows the CRLB. This result opens an opportunity for the application of chaos and symbolic dynamics for improving blind system identification.

Our goal is to develop a technique for blind channel equalization for improving wireless communication by our proposed method. Hence, we have evaluated our technique using AR and MA models as they are popular models in communication. We then validated our method using experimentation with a real dataset collected from software defined radio (SDR) and applied our method for blind equalization of a channel where the MA components represent a finite impulse response and is modeled as a FIR system. Using SDR, the proposed method is also shown to have superior performance compared to HOS based blind methods. Based on our analysis, we can infer that chaotic signals either in numeric or symbolic format can act as an ideal candidate for blind system identification using our proposed ML-PSV method. Apart from chaos-based equalization application which we have presented in our work, we could also apply the ML-PSV estimator in narrow-band interference cancellation for spread spectrum communications and in chaos-based pulse amplitude modulated (CPAM) UWB radar. The chaos-based UWB radar finds its application in through-wall imaging for detection.

REFERENCES

[1] G. Chen, Y. Chen, and H. Ogmen, "Identifying chaotic systems via a Wiener-type cascade model," *IEEE Control Syst.*, vol. 17, no. 5, pp. 29–36, Oct. 1997.

[2] L. Vanbeylen, R. Pintelon, and J. Schoukens, "Application of blind identification to nonlinear calibration," *IEEE Trans. Instrum. Meas.*, vol. 57, no. 8, pp. 1771–1778, Aug. 2008.

[3] K. Abed-Meraim, P. Loubaton, and E. Moulines, "A subspace algorithm for certain blind identification problems," *IEEE Trans. Inf. Theory*, vol. 43, no. 2, pp. 499–511, Mar. 1997.

[4] C.-Y. Chi, C.-C. Feng, C. Chii-Horng, and C.-Y. Chen, *Blind Equalization and System Identification: Batch Processing Algorithms, Performance and Applications*. Cham, Switzerland: Springer, 2006.

[5] L. R. Litwin, "Blind channel equalization," *IEEE Potentials*, vol. 18, no. 4, pp. 9–12, Oct. 1999.

[6] X. Li and J. Wang, "Robust blind identification algorithm in stationary noise environments," *IET Commun.*, vol. 14, no. 2, pp. 313–319, Jan. 2020.

[7] J. Ma, T. Qiu, and Q. Tian, "Fast blind equalization using bounded nonlinear function with non-Gaussian noise," *IEEE Commun. Lett.*, vol. 24, no. 8, pp. 1812–1815, Aug. 2020.

[8] Y.-W. Chen, S. Narieda, and K. Yamashita, "Blind nonlinear system identification based on a constrained hybrid genetic algorithm," *IEEE Trans. Instrum. Meas.*, vol. 52, no. 3, pp. 898–902, Jun. 2003.

[9] H. Leung, "System identification using chaos with application to equalization of a chaotic modulation system," *IEEE Trans. Circuits Syst. I, Fundam. Theory Appl.*, vol. 45, no. 3, pp. 314–320, Mar. 1998.

[10] V. Venkatasubramanian and H. Leung, "An EM based method for semi blind identification of linear systems driven by chaotic signals," in *Proc. IEEE Conf. Cybern. Intell. Syst.*, vol. 1, Dec. 2004, pp. 554–557.

[11] H. Leung, *Chaotic Signal Processing*, vol. 136. Philadelphia, PA, USA: SIAM, 2013.

[12] S. Mukhopadhyay and H. Leung, "Blind system identification using symbolic dynamics," *IEEE Access*, vol. 6, pp. 24888–24903, 2018.

[13] Q. Han, L. Yang, J. Du, and L. Cheng, "Blind equalization for chaotic signals based on echo state network and Kalman filter under nonlinear channels," *IEEE Commun. Lett.*, early access, Oct. 20, 2020, doi: 10.1109/LCOMM.2020.3032587.

[14] G. Kaddoum, M. Vu, and F. Gagnon, "Performance analysis of differential chaotic shift keying communications in MIMO systems," in *Proc. IEEE Int. Symp. Circuits Syst. (ISCAS)*, May 2011, pp. 1580–1583.

[15] H.-P. Ren, M. S. Baptista, and C. Grebogi, "Wireless communication with chaos," *Phys. Rev. Lett.*, vol. 110, no. 18, Apr. 2013, Art. no. 184101.

[16] H. Leung, S. Shanmugam, N. Xie, and S. Wang, "An ergodic approach for chaotic signal estimation at low SNR with application to ultra-wideband communication," *IEEE Trans. Signal Process.*, vol. 54, no. 3, pp. 1091–1103, Mar. 2006.

[17] C. Vural and G. Çetinel, "Blind equalization of single-input single-output fir channels for chaotic communication systems," *Digit. Signal Process.*, vol. 20, no. 1, pp. 201–211, Jan. 2010.

[18] G. Kaddoum, "Wireless chaos-based communication systems: A comprehensive survey," *IEEE Access*, vol. 4, pp. 2621–2648, 2016.

[19] X. Xu, J. Guo, and H. Leung, "Blind equalization for power-line communications using chaos," *IEEE Trans. Power Del.*, vol. 29, no. 3, pp. 1103–1110, Jun. 2014.

[20] T. Carroll, "Chaotic control and synchronization for system identification," *Phys. Rev. E, Stat. Phys. Plasmas Fluids Relat. Interdiscip. Top.*, vol. 69, no. 4, Apr. 2004, Art. no. 046202.

[21] D. Rontani, A. Locquet, M. Sciamanna, D. S. Citrin, and S. Ortin, "Time-delay identification in a chaotic semiconductor laser with optical feedback: A dynamical point of view," *IEEE J. Quantum Electron.*, vol. 45, no. 7, pp. 1879–1891, Jul. 2009.

[22] S. Mukhopadhyay and H. Leung, "Cluster synchronization of predator prey robots," in *Proc. IEEE Int. Conf. Syst., Man, Cybern.*, Oct. 2013, pp. 2753–2758.

[23] S. Mukhopadhyay and H. Leung, "Dynamical systems approach for predator-prey robot behavior control via symbolic dynamics based communication," in *Encyclopedia of Information Science and Technology*, 3rd ed. Hershey, PA, USA: IGI Global, 2015, pp. 6621–6632.

[24] L. M. Pecora and T. L. Carroll, "Synchronization of chaotic systems," *Chaos, Interdiscipl. J. Nonlinear Sci.*, vol. 25, no. 9, Sep. 2015, Art. no. 097611, doi: 10.1063/1.4917383.

[25] N. Xie and H. Leung, "Blind identification of autoregressive system using chaos," *IEEE Trans. Circuits Syst. I, Reg. Papers*, vol. 52, no. 9, pp. 1953–1964, Sep. 2005.

[26] S. Kay and V. Nagesha, "Methods for chaotic signal estimation," *IEEE Trans. Signal Process.*, vol. 43, no. 8, pp. 2013–2016, Aug. 1995.

[27] I. Hen and N. Merhav, "On the threshold effect in the estimation of chaotic sequences," *IEEE Trans. Inf. Theory*, vol. 50, no. 11, pp. 2894–2904, Nov. 2004.

[28] D. He and H. Leung, "Semi-blind identification of ARMA systems using a dynamic-based approach," *IEEE Trans. Circuits Syst. I, Reg. Papers*, vol. 52, no. 1, pp. 179–190, Jan. 2005.

[29] H. Leung, S. Wang, and A. M. Chan, "Blind identification of an autoregressive system using a nonlinear dynamical approach," *IEEE Trans. Signal Process.*, vol. 48, no. 11, pp. 3017–3027, 2000.
[30] Z. Zhu and H. Leung, "Identification of linear systems driven by chaotic signals using nonlinear prediction," *IEEE Trans. Circuits Syst. I, Fundam. Theory Appl.*, vol. 49, no. 2, pp. 170–180, 2002.
[31] H. Leung and X. Huang, "Parameter estimation in chaotic noise," *IEEE Trans. Signal Process.*, vol. 44, no. 10, pp. 2456–2463, 1996.
[32] A. Kurian and H. Leung, "System identification using chaos," in *Chaotic Signal Processing*, H. Leung, Ed. Philadelphia, PA, USA: SIAM, 2014, ch. 5.
[33] D. Luengo, I. Santamaría, and L. Vielva, "Asymptotically optimal maximum-likelihood estimation of a class of chaotic signals using the Viterbi algorithm," in *Proc. 13th Eur. Signal Process. Conf.*, Sep. 2005, pp. 1–4.
[34] G. Kaddoum, F. Gagnon, and D. Couillard, "An enhanced spectral efficiency chaos-based symbolic dynamics transceiver design," in *Proc. 6th Int. Conf. Signal Process. Commun. Syst.*, Dec. 2012, pp. 1–6.
[35] J. Schweizer and T. Schimming, "Symbolic dynamics for processing chaotic signals. I. Noise reduction of chaotic sequences," *IEEE Trans. Circuits Syst. I, Fundam. Theory Appl.*, vol. 48, no. 11, pp. 1269–1282, 2001.
[36] C. S. Daw, C. E. A. Finney, and E. R. Tracy, "A review of symbolic analysis of experimental data," *Rev. Sci. Instrum.*, vol. 74, no. 2, pp. 915–930, Feb. 2003.
[37] N. Wessel, C. Ziehmann, J. Kurths, U. Meyerfeldt, A. Schirdewan, and A. Voss, "Short-term forecasting of life-threatening cardiac arrhythmias based on symbolic dynamics and finite-time growth rates," *Phys. Rev. E, Stat. Phys. Plasmas Fluids Relat. Interdiscip. Top.*, vol. 61, no. 1, p. 733, 2000.
[38] S. Mukhopadhyay and H. Leung, "Recognizing human behavior through nonlinear dynamics and syntactic learning," in *Proc. IEEE Int. Conf. Syst., Man, Cybern. (SMC)*, Oct. 2012, pp. 846–850.
[39] S. Kay, "Asymptotic maximum likelihood estimator performance for chaotic signals in noise," *IEEE Trans. Signal Process.*, vol. 43, no. 4, pp. 1009–1012, Apr. 1995.
[40] I. Kollar and Y. Rolain, "Complex correction of data acquisition channels using FIR equalizer filters," *IEEE Trans. Instrum. Meas.*, vol. 42, no. 5, pp. 920–924, Oct. 1993.
[41] Z. Ding and Z.-Q. Luo, "A fast linear programming algorithm for blind equalization," *IEEE Trans. Commun.*, vol. 48, no. 9, pp. 1432–1436, Sep. 2000.
[42] Z. Xie, X. Chen, and X. Liu, "Joint channel estimation and equalization for MIMO-SCFDE systems over doubly selective channels," *J. Commun. Netw.*, vol. 19, no. 6, pp. 627–636, Dec. 2017.
[43] K. Hwang and S. Choi, "Blind equalization method based on sparse Bayesian learning," *IEEE Signal Process. Lett.*, vol. 16, no. 4, pp. 315–318, Apr. 2009.
[44] D. Hatzinakos and C. L. Nikias, "Blind equalization using a tricepstrum-based algorithm," *IEEE Trans. Commun.*, vol. 39, no. 5, pp. 669–682, May 1991.
[45] Q. Mayyala, K. Abed-Meraim, and A. Zerguine, "Structure-based subspace method for multichannel blind system identification," *IEEE Signal Process. Lett.*, vol. 24, no. 8, pp. 1183–1187, Aug. 2017.
[46] S. J. Qin, "An overview of subspace identification," *Comput. Chem. Eng.*, vol. 30, nos. 10–12, pp. 1502–1513, Sep. 2006.
[47] F. Takens, "Detecting strange attractors in turbulence," in *Dynamical Systems and Turbulence, Warwick 1980*. Cham, Switzerland: Springer, 1981, pp. 366–381.
[48] H. Kantz and T. Schreiber, *Nonlinear Time Series Analysis*, vol. 7. Cambridge, U.K.: Cambridge Univ. Press, 2004,
[49] G. Kember and A. C. Fowler, "A correlation function for choosing time delays in phase portrait reconstructions," *Phys. Lett. A*, vol. 179, no. 2, pp. 72–80, Aug. 1993.
[50] E. Levina and P. J. Bickel, "Maximum likelihood estimation of intrinsic dimension," in *Proc. Adv. Neural Inf. Process. Syst.*, 2005, pp. 777–784.
[51] M. Casdagli, S. Eubank, J. D. Farmer, and J. Gibson, "State space reconstruction in the presence of noise," *Phys. D, Nonlinear Phenomena*, vol. 51, nos. 1–3, pp. 52–98, Aug. 1991.
[52] A. Torre, "1—Hamiltonian picture of light optics. First-order ray optics," in *Linear Ray and Wave Optics in Phase Space*, A. Torre, Ed. Amsterdam, The Netherlands: Elsevier, 2005, pp. 1–58. [Online]. Available: http://www.sciencedirect.com/science/article/pii/B9780444517999500017

SUMONA MUKHOPADHYAY received the Ph.D. degree in electrical and computer engineering from the University of Calgary, AB, Canada in 2018. After completing her Ph.D. degree, she was a Postdoctoral Associate with the System Identification Lab, University of Calgary, from 2018 to 2019. She was an Alberta Innovates Technology Futures (AITF) Doctoral Scholar. She is currently a Postdoctoral Fellow with the Adaptive Software Research Laboratory, York University, ON, Canada. Her research interests include optimization, signal processing, artificial intelligence, predictive analytics, and data mining.

BOYUAN LI received the bachelor's and master's degrees in communication engineering from Nanchang University, China, in 2011 and 2014, respectively. He is currently pursuing the Ph.D. degree with the Department of Electrical and Computer Engineering, University of Calgary, Canada. His research interests include wireless communication, software-defined radio, and the IoT.

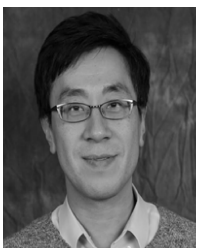

HENRY LEUNG (Fellow, IEEE) was with the Department of National Defence (DND) of Canada as a Defence Scientist. He is currently a Professor with the Department of Electrical and Computer Engineering, University of Calgary. His current research interests include information fusion, machine learning, nonlinear dynamics, robotics, and signal and image processing. He is a fellow of SPIE. He is also an Associate Editor of the *IEEE Circuits and Systems Magazine*. He is the Topic Editor on "Robotic Sensors" of the *International Journal of Advanced Robotic Systems*. He is an Editor of *Information Fusion and Data Science* (Springer book series).